

Instrument Science Report ACS 2007-09

Two astrometric fields for UV observations

Jesús Maíz Apellániz

Instituto de Astrofísica de Andalucía-CSIC

27 August 2007

REVISED: 4 October 2007

ABSTRACT

I present the data for two fields that can be used to obtain accurate astrometric calibrations in the UV. The two fields are located in NGC 604 (a Scaled OB Association in M33) and NGC 6681 (a Galactic globular cluster). The coordinates are derived from multiple ACS/HRC exposures, use the Anderson and King (2004) geometric distortion solution, have typical relative uncertainties of 1 mas, and can be used to derive geometric distortion solutions for detectors with a field of view smaller than 1'. In the process of generating the astrometric fields, the long-term stability of the HRC geometric distortion solution has been successfully tested. In two future ISRs these results will be used to derive new geometric distortion solutions for the STIS NUV- and FUV-MAMA and for the ACS SBC.

Introduction

The high degree of photometric, astrometric, and spectrophotometric precision that can be attained with HST has generated the need for several new calibration techniques, models, and standard objects. Given the difficulty of finding non-HST data with the desired properties for such calibration tasks, one often has to resort to self-calibration. In this Instrument Science Report I present the data for two fields that can be used to derive or to test the geometric distortion of an imaging UV detector.

The coordinates for the two fields were derived from multiple ACS/HRC UV images that were processed using JMAPHOT, a crowded-field photometry package designed specifically for the HRC. The positions in the

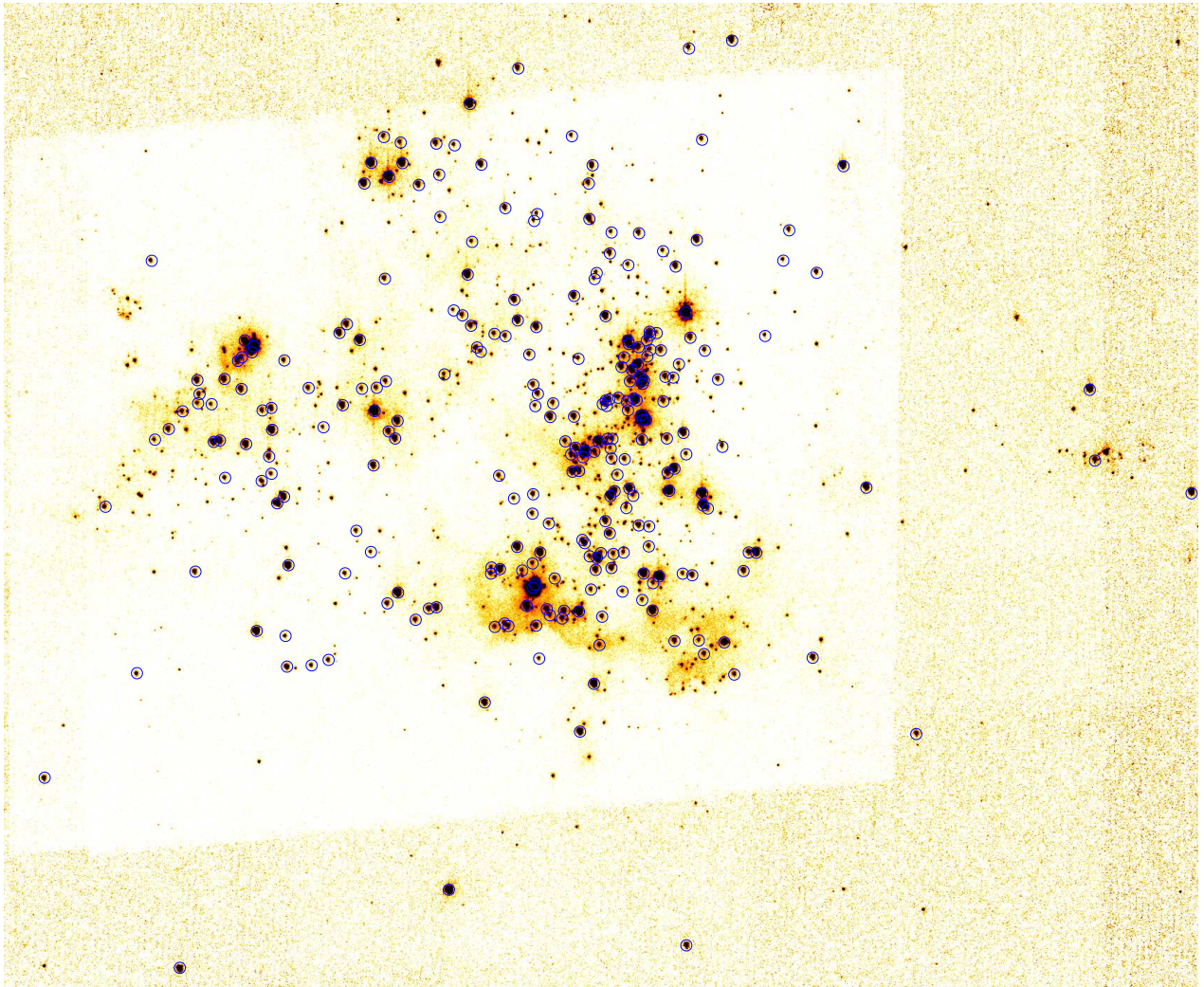


Figure 1: F250W DRZ mosaic of the NGC 604 field. The stars in Table 3 are marked with blue circles. The field is centered at $1^{\text{h}} 34^{\text{m}} 32^{\text{s}}.7088$, $30^{\circ} 47' 5''.501$, has a size of $42''.5 \times 35''.0$, and the vertical direction is 49° East of North. The total exposure time is 2288 s.

detector were corrected using the Anderson and King (2004) geometric distortion solution for the HRC, which was derived using multiple observations of the globular cluster 47 Tuc applying a self-calibration technique. That solution is extremely accurate for an ideal case (positions measured in a dense field with a single orientation, a single epoch, and with certain filters), yielding uncertainties of ~ 0.005 pixels (0.125 mas) for stars with $S/N = 1000$, ~ 0.02 pixels (0.5 mas) for stars with $S/N = 100$, and ~ 0.1 pixels (2.5 mas) for stars with $S/N = 30$. The geometric distortion has two components: a polynomial fit common to all filters and a lookup table which is filter dependent. Most of the distortion is contained in the polynomial fit, with the filter-dependent tables introducing corrections of the order of only 0.05 pixels. Anderson and King (2004) did not provide filter-dependent tables for all filters: in the UV they do it for F220W (note that there is a typo in their tables 2 and 4 that misidentifies this filter as F250W) but not for F250W. Therefore, one would expect the latter filter to yield somewhat larger uncertainties than the former. Another point made by Anderson and King (2004) is the possibility of frame-to-frame variations in the linear terms of the polynomial component: their recom-

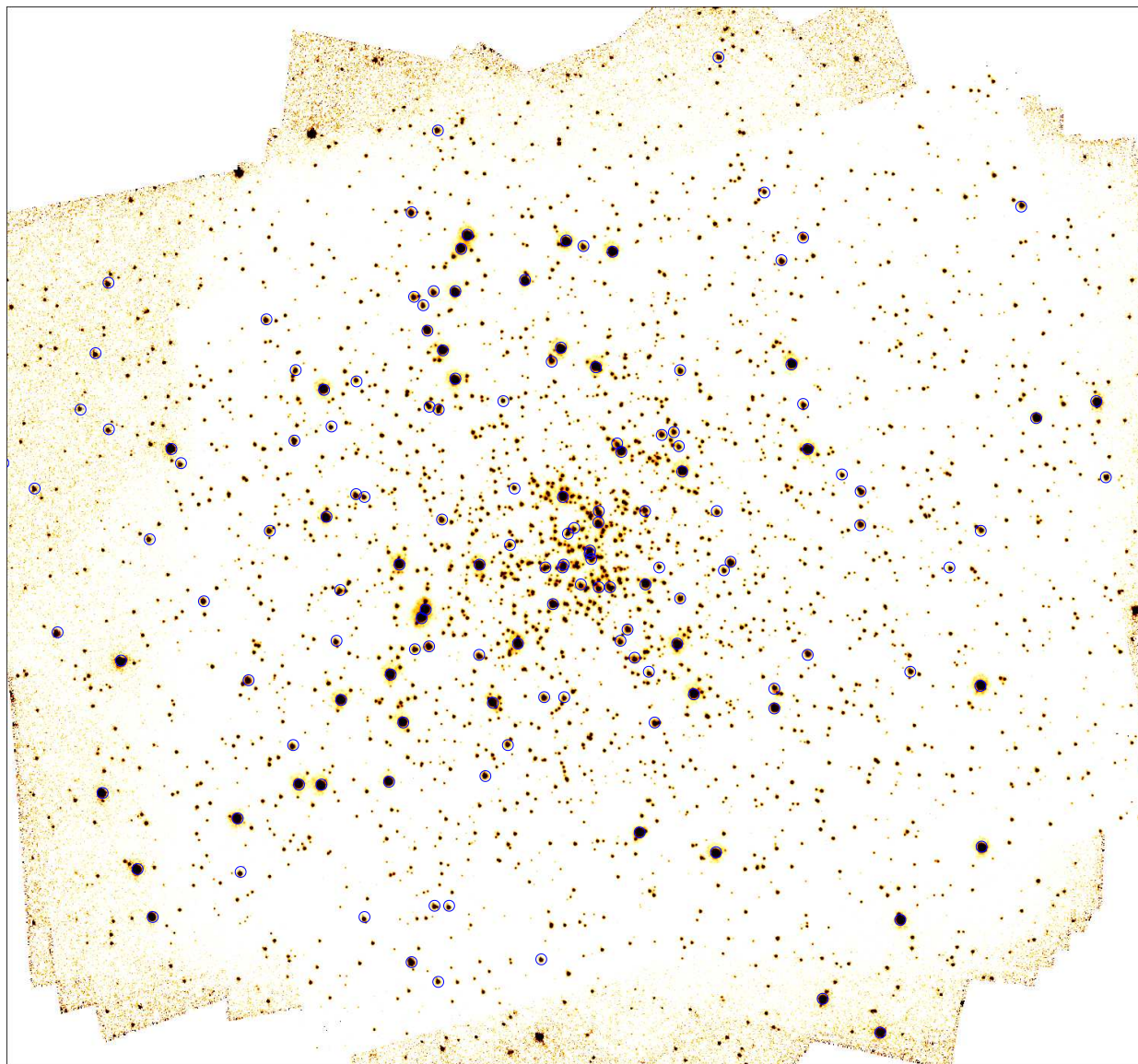


Figure 2: F250W DRZ mosaic of the NGC 6681 field. The stars in Table 4 are marked with blue circles. The field is centered at $18^{\text{h}} 43^{\text{m}} 12^{\text{s}}.6415$, $-32^{\circ} 17' 31''.161$, has a size of $37''.5 \times 35''.0$, and the vertical direction is 270° East of North. The total exposure time is 6260 s.

mended strategy is to fit those six terms for each frame using independent information (e.g. external accurate coordinates or multiple frames).

As described in the following section, the datasets used in this ISR do not correspond to the ideal case in the above paragraph: the observations were done in moderately crowded fields with tens or hundreds (but not thousands) of bright sources, in one of the two fields there were multiple orientations and epochs, some of the frames were obtained with F250W, and the typical S/N for a bright star was closer to 100 than to 1000. On the other hand, many frames are available for each field, which allows for an independent characterization of the uncertainties associated with the HRC geometric distortion solution, including its long term stability.

Data

The data for the two fields in this report are described below.

NGC 604

NGC 604 is a Scaled OB Association (SOBA) in M33 located at a distance of 840 kpc that was first observed with an HST imager by Drissen et al. (1993) using WFPC1. Subsequent HST imaging is described in Hunter et al. (1996) (WFPC2), Maíz Apellániz and Úbeda (2004) (WFPC2 and STIS/NUV-MAMA), and Maíz Apellániz et al. (2004) (WFPC2). It has ~ 200 O+WR stars (Hunter et al. 1996) as well as several hundred bright-B stars (Fig. 1), most of them located within $13''$ of the center of a low-extinction cavity (Maíz Apellániz et al. 2004). The brightest sources have NUV ST magnitudes of 14-15. HST UV images of NGC 604 can be classified as moderately crowded.

The ACS/HRC NGC 604 images used in this ISR were acquired under two HST programs, GO 10419 (P.I.: R. Barbá) and CAL 10722, using two filters, F220W and F250W. A total of 20 exposures/filter were obtained, each with the same orientation (within 1°) but using a mosaic dithering pattern to allow a given star to fall in different parts of the CCD. The eight GO 10419 exposures (listed first in Table 1) were slightly longer (150 s and 200 s for F220W and F250W, respectively) than the thirty-two CAL 10722 ones (87 s and 93 s for F220W and F250W, respectively). As a result of this strategy, the central region of NGC 604, where most of the UV-bright stars are located, was observed for longer accumulated exposure times than the surrounding area, as it can be seen by the different S/N ratios of the background in Fig. 1. All exposures were obtained on 14 September 2005. In a single exposure, S/N ratios of ≈ 200 and 300 were obtained for the brightest stars in F220W and F250W, respectively. For late-O/early-B main sequence stars the corresponding values were 30 and 40 for F220W and F250W, respectively.

Table 1. NGC 604 datasets.

| F220W | | F250W | |
|-----------|-----------|-----------|-----------|
| j96y11g9q | j9hn03f6q | j96y11gaq | j9hn03fsq |
| j96y11ggq | j9hn03f8q | j96y11ghq | j9hn03ftq |
| j96y11goq | j9hn03f9q | j96y11gpq | j9hn03fuq |
| j96y11gvq | j9hn03fbq | j96y11gwq | j9hn03fvq |
| j9hn03eyq | j9hn03fcq | j9hn03flq | j9hn03fwq |
| j9hn03ezq | j9hn03feq | j9hn03fnq | j9hn03fxq |
| j9hn03f0q | j9hn03ffq | j9hn03foq | j9hn03fyq |
| j9hn03f2q | j9hn03fhq | j9hn03fpq | j9hn03fzq |
| j9hn03f3q | j9hn03fiq | j9hn03fqq | j9hn03g0q |
| j9hn03f5q | j9hn03fkq | j9hn03frq | j9hn03g1q |

NGC 6681

NGC 6681 is a Galactic globular cluster located at a distance of 9 kpc (Harris 1996). It has been repeatedly observed with HST, since it has been used for calibration purposes for a number of HST instruments, including the four UV detectors on STIS and ACS. Its UV-bright population is quite different from NGC 604: in the FUV the luminosity is dominated by several tens of white-dwarf containing systems, with the rest of the stars in the cluster contributing only a small percentage of the measured flux. Therefore, the HST FUV images

of NGC 6681 are quite sparse, even at the center of the cluster. As we move towards longer wavelengths we start to detect main sequence stars, blue stragglers, and horizontal branch stars and, as a result, U -band (e.g HRC F330W) images are already severely crowded near the center of NGC 6681. The brightest UV stars in NGC 6681 have NUV ST magnitudes of 15-16.

Table 2. NGC 6681 datasets.

| F220W | | | F250W | | |
|-----------|-----------|-----------|-----------|-----------|-----------|
| j8bt10qtq | j8ep07v3q | j8hv12dkq | j8c601tmq | j8ep08lkq | j8vb01ocq |
| j8bt10quq | j8ep07v4q | j8hv12dlq | j8c601u9q | j8ep08llq | j8vb01odq |
| j8bt10qvq | j8ep08liq | j8vb01oaq | j8c801mrq | j8hv01lqq | j8vb03eaq |
| j8bt10qwq | j8ep08ljq | j8vb01obq | j8c801msq | j8hv01lrq | j8vb03ebq |
| j8c801mpq | j8hv01loq | j8vb03e8q | j8c803hkq | j8hv02euq | j8vb05ynq |
| j8c801mq | j8hv01lpq | j8vb03e9q | j8c803hlq | j8hv02evq | j8vb05yoq |
| j8c803hiq | j8hv02esq | j8vb05ylq | j8c804w0q | j8hv05byq | j8vb07exq |
| j8c803hj | j8hv02etq | j8vb05ymq | j8c804w1q | j8hv05bzq | j8vb07eyq |
| j8c804vyq | j8hv05bwq | j8vb07evq | j8ep01tts | j8hv06qh | j95u01jyq |
| j8c804vzq | j8hv05bxq | j8vb07ewq | j8ep01tus | j8hv06qiq | j95u01jzq |
| j8ep01trs | j8hv06qfq | j95u01jwq | j8ep02uoq | j8hv07oxq | j9i001e6q |
| j8ep01tss | j8hv06qgq | j95u01jxq | j8ep02upq | j8hv07oyq | j9i001e7q |
| j8ep02umq | j8hv07ovq | j9i001e4q | j8ep03g8q | j8hv08s9q | j9i001ecq |
| j8ep02unq | j8hv07owq | j9i001e5q | j8ep03g9q | j8hv08saq | j9i001edq |
| j8ep03g6q | j8hv08s7q | j9i001eaq | j8ep04llq | j8hv09yqq | j9i002s7q |
| j8ep03g7q | j8hv08s8q | j9i001ebq | j8ep04lmq | j8hv09yrq | j9i002s8q |
| j8ep04lj | j8hv09yoq | j9i002s5q | j8ep05piq | j8hv10cdq | j9i002sdq |
| j8ep04lkq | j8hv09ypq | j9i002s6q | j8ep05pj | j8hv10ceq | j9i002seq |
| j8ep05pgq | j8hv10cbq | j9i002sbq | j8ep06hfq | j8hv11a1q | |
| j8ep05phq | j8hv10ccq | j9i002scq | j8ep06hgq | j8hv11a2q | |
| j8ep06hdq | j8hv11zyq | | j8ep07v5q | j8hv12dmq | |
| j8ep06heq | j8hv11zzq | | j8ep07v6q | j8hv12dnq | |

NGC 6681 has been observed with ACS/HRC using its two UV continuum filters (F220W and F250W) under seven different calibration programs: 9019, 9023, 9010, 9565, 9655, 10047, 10373, and 10736¹. A total of 64 and 62 datasets are available for F220W and F250W, respectively (Table 2). The observations in the two filters span from the spring of 2002 to the spring of 2006 to cover almost four years. Most of the datasets have exposure times of 70 s with the following exceptions: (a) The first four datasets for F220W (CAL 9019) have exposure times of 340 s. (b) The first two datasets for F250W (CAL 9023) have exposure times of 1200 s. (c) The last eight datasets in all filters (CAL 10736) have exposure times of 35 s and 27.5 s for F220W and F250W, respectively. The exposures in each filter were obtained with a variety of orientations and dithering strategies. The cluster core appears in all exposures but, as we move outwards, the accumulated exposure time for a given location decreases, as is easily seen in the S/N ratio of the background in Fig. 2. In the 70 s exposures one typically finds 50 bright stars with S/N ratios between 50 and 80 (F220W) and 70 and 100 (F250W); the rest of the point sources do not include white dwarfs and are considerably dimmer.

¹The U -band HRC equivalent, F330W, was also included in those programs, but is not used in this ISR.

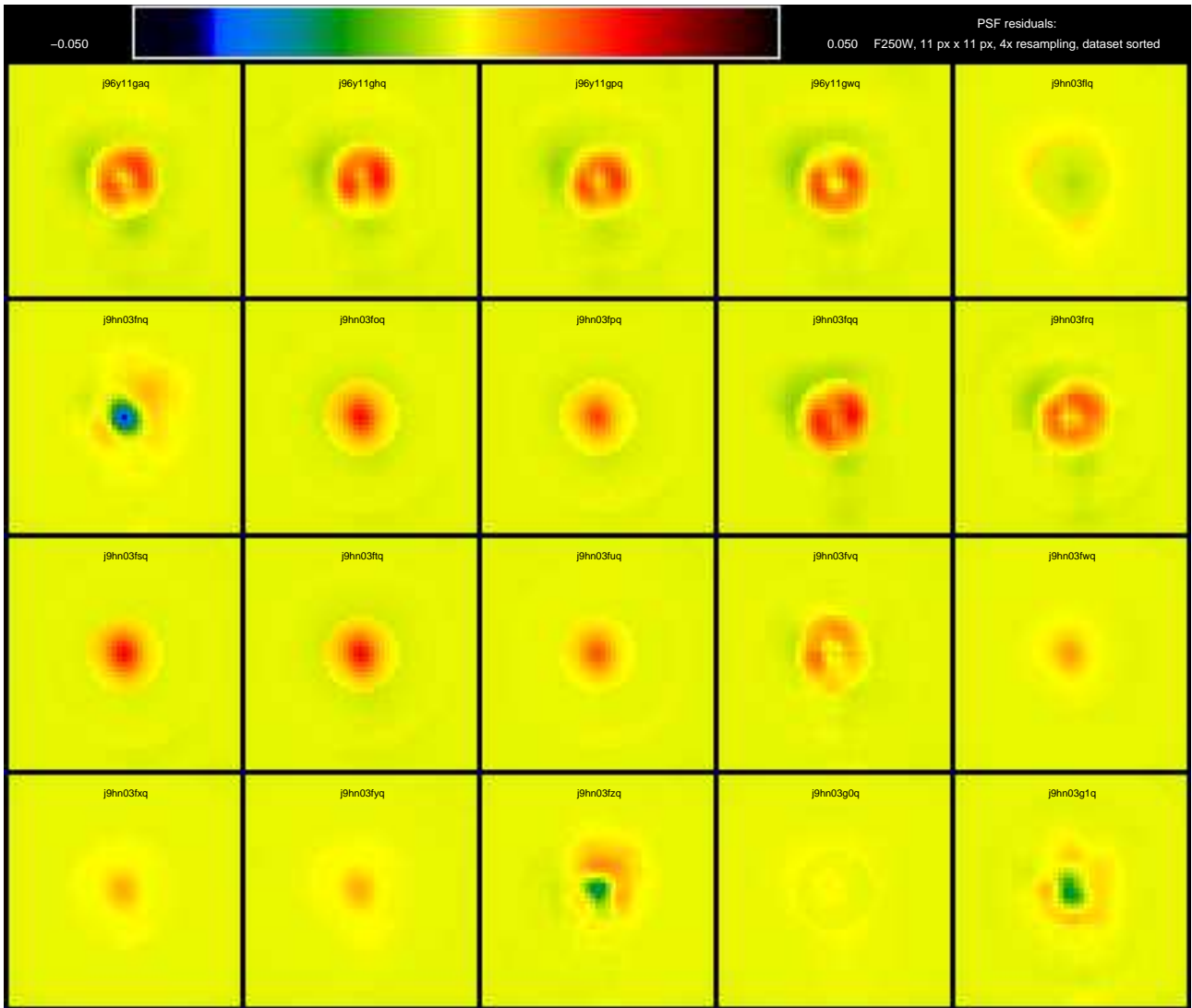


Figure 3: ePSF residuals for the 20 F250W NGC 604 frames. The residuals are calculated every quarter of a pixel and are normalized with respect to the total PSF flux, with a range that spans between -0.05 and 0.05 pixel^{-1} . For example, a value of 0.03 pixel^{-1} implies that the residual at a pixel centered at that location has 3% of the total flux in the ePSF.

Technique

The data were processed using JMAPHOT, a crowded-field photometry package that I have written for the specific goal of analyzing multiple ACS/HRC and STIS imaging exposures of a given field. Each of the four combinations of object+filter (NGC 604 - F220W, NGC 604 - F250W, NGC 6681 - F220W, and NGC 6681 - F250W) had all their datasets (20, 20, 64, and 62 respectively) processed simultaneously. The steps used were the following:

- An initial search and classification (as cosmic rays, extended, or point-like) of sources was performed in each FLT frame (cosmic-ray + hot pixel “dirty”, uncorrected for geometric distortion). The point sources

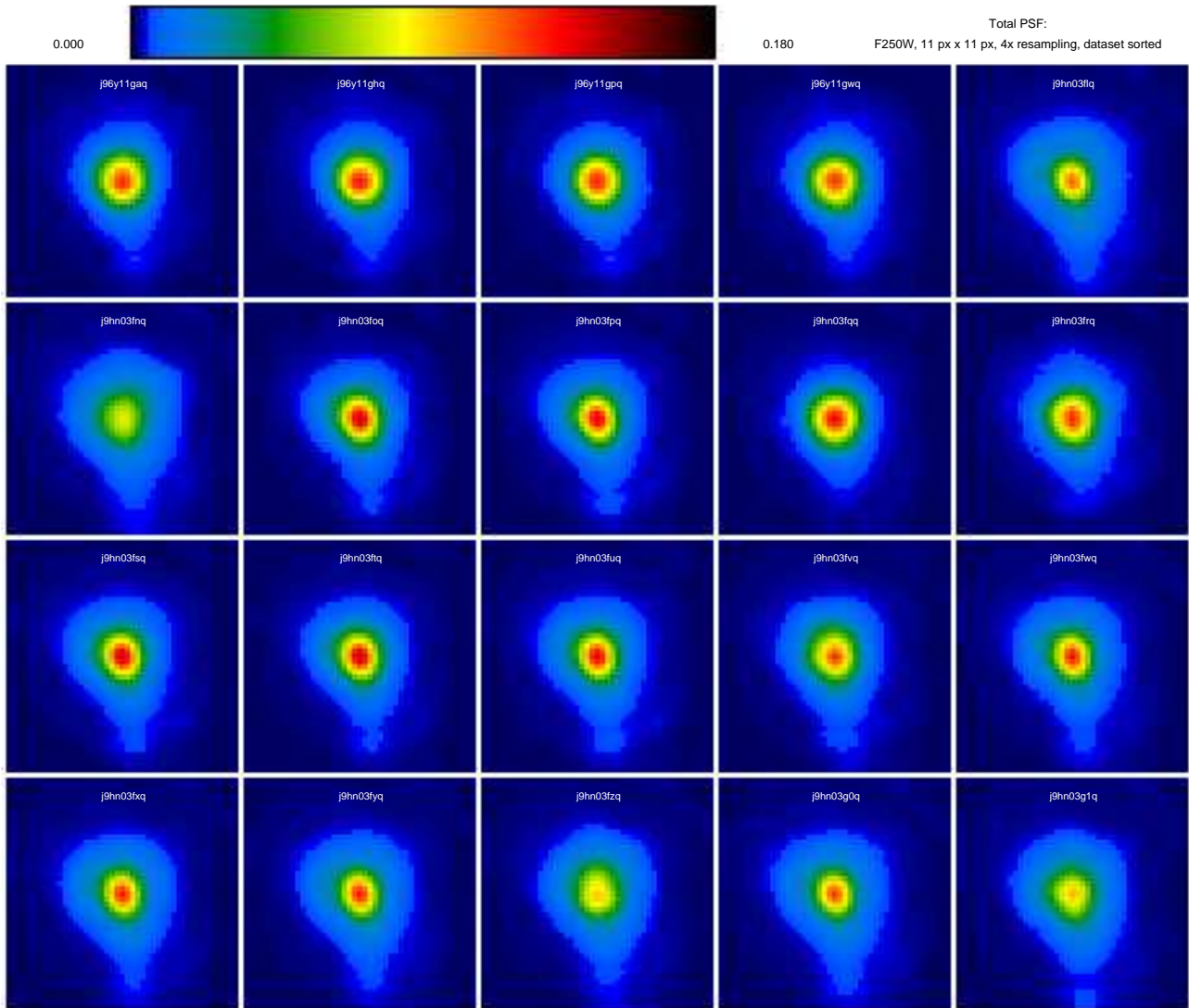


Figure 4: Total ePSFs (original ePSF + residual) for the 20 F250W NGC 604 frames. The ePSFs are calculated every quarter of a pixel and are normalized with respect to the total PSF flux, with a range that spans between 0.00 and 0.18 pixel^{-1} . For example, a value of 0.07 pixel^{-1} implies that the ePSF at a pixel centered at that location has 7% of the total flux. Given the $4\times$ oversampling, the sum of all points in one of the ePSFs (if extended to infinity) is 16.

were used to build a preliminary catalog for each frame which was then correlated with the other frames for the same object+filter in order to calculate the initial estimates for the relative displacements between frames. Those initial estimates use the standard average geometric distortion (i.e. they do not take into account possible variations in the linear terms) and allow for the calculation of positions with ~ 0.1 pixel accuracy, which is enough for the generation of a DRZ mosaic (cosmic-ray + hot pixel “cleaned”, corrected for geometric distortion) by combining all the frames.

- Multidrizzle was used with the displacements calculated above to generate the high-S/N-ratio DRZ mosaic with all the data for each combination of object+filter, as well as the SCI_COR version of each FLT

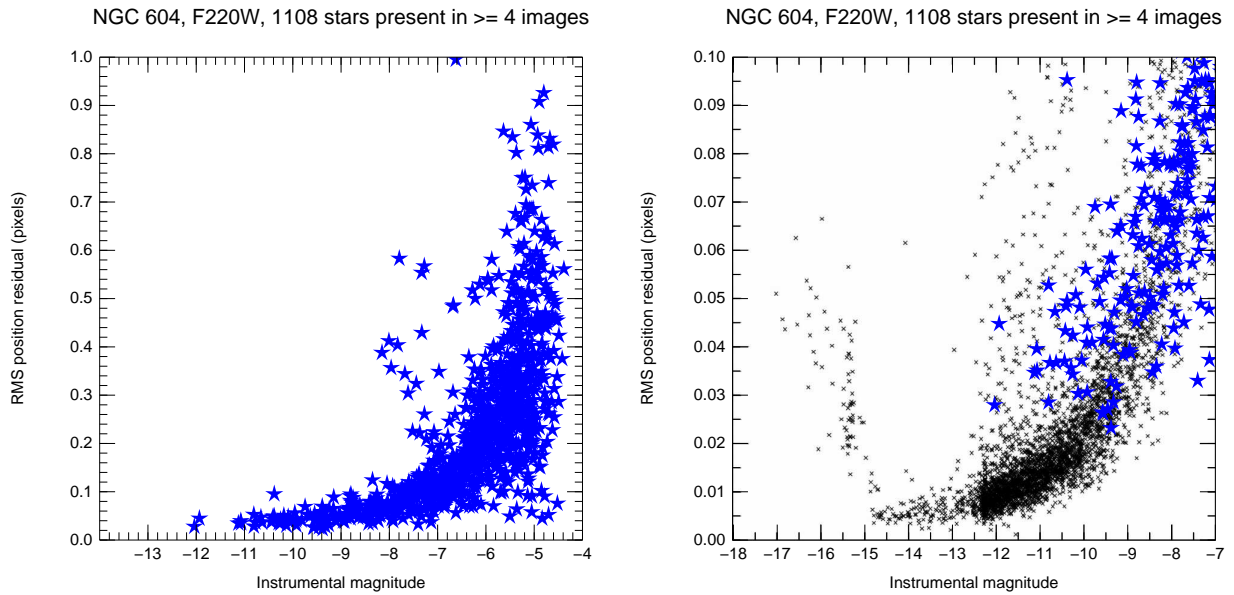


Figure 5: RMS position residuals for the NGC 604 stars present in at least four F220W exposures. The left panel shows most of the detected stars (a few very dim stars have values larger than 1 pixel). The right panel is a blow-up of the left-hand corner, adding the data given by Anderson & King (2004) for F475W in black. 1 DRZ pixel = 25 mas. The instrumental magnitude, m_{ins} , is defined as $-2.5 \log_{10}(\text{electrons})$, refers to an exposure time of 87 s, and is uncorrected for quantum-yield effects (see subsection 4.3.8 in the ACS Instrument Handbook). Note that the Anderson & King (2004) data are saturated for stars brighter than -14.75 .

frame. The SCI_COR frames are not corrected for geometric distortion but are cleaned of cosmic rays and hot pixels.

- A search for sources was performed on the DRZ mosaic and the initial estimates for the displacements were used to transform the coordinates into each SCI_COR (or FLT) frame. Again, the accuracy of those positions is expected to be ~ 0.1 pixels.
- The background was calculated for each SCI_COR frame. For NGC 6681 a simple constant background was used. For NGC 604 a variable background was needed because of the existence of nebulosity (visible in Fig. 1).
- The positions and fluxes of all sources in each SCI_COR frame were simultaneously fit using an ePSF that has an Anderson and King (2004) core and Tiny Tim wings. The used ePSF was oversampled by a factor of 4.
- A PSF residual was calculated for each frame (Figs. 3 and 4) and the positions and fluxes of all sources in each SCI_COR frame were fitted again using the resulting PSF².
- The final positions for every star in all frames were combined into an average position by using the Anderson and King (2004) geometric distortion solution and fitting the linear terms of the transformation

²This is essentially the same idea discussed in Anderson and King (2006).

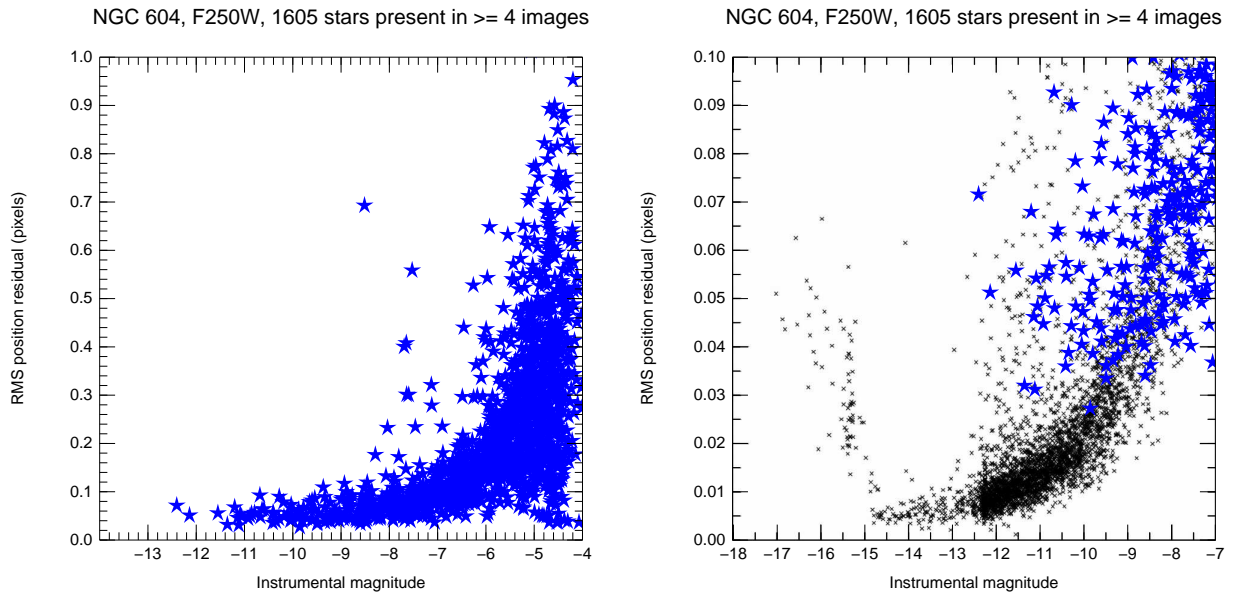


Figure 6: Same as Fig. 5 for NGC 604 and F250W exposures. The instrumental magnitude refers to an exposure time of 70 s.

for each frame using a χ^2 minimization algorithm. The process was first executed using a given frame as a reference and then iterated once the average positions of each star had been calculated.

Results

In order to combine the frames into an average position, I selected those stars that were present in a minimum number of exposures (4 for NGC 604, 6 for NGC 6681), and calculated their position uncertainties³ from the RMS values in x and y . The position residuals are shown in Figs. 5 to 8 as a function of the instrumental magnitude, m_{ins} , defined as $-2.5 \log_{10}(\text{electrons})$. The right panels show a detail of the left ones with the F435W Anderson and King (2004) results in the background. For NGC 6681, where the frames have a large variation in orientation, I also calculated the RMS position residuals by comparing pairs of consecutive exposures taken with the same orientation and within the same visit: this allowed me to separate the uncertainties caused by S/N effects and the fitting procedure from those caused by possible issues with the geometric distortion solution and/or its temporal evolution. Note that the F475W Anderson and King (2004) results were obtained with different position offsets but with the same orientation and epoch.

Overall, I can reproduce most of the Anderson and King (2004) results: the RMS position residuals are ≈ 0.1 pixel for S/N ratios of 30 ($m_{\text{ins}} \approx -7.5$) and the same general shape as a function of m_{ins} is also observed. However, some differences are also present:

- For the NGC 6681 F220W data, the stars have uncertainties of ≈ 0.1 pixel for $m_{\text{ins}} < -7.5$ with little dependence on S/N. For the other three cases there is a significant reduction in the uncertainties as m_{ins}

³These uncertainties do not refer to an absolute reference frame but to a relative one (see below for details).

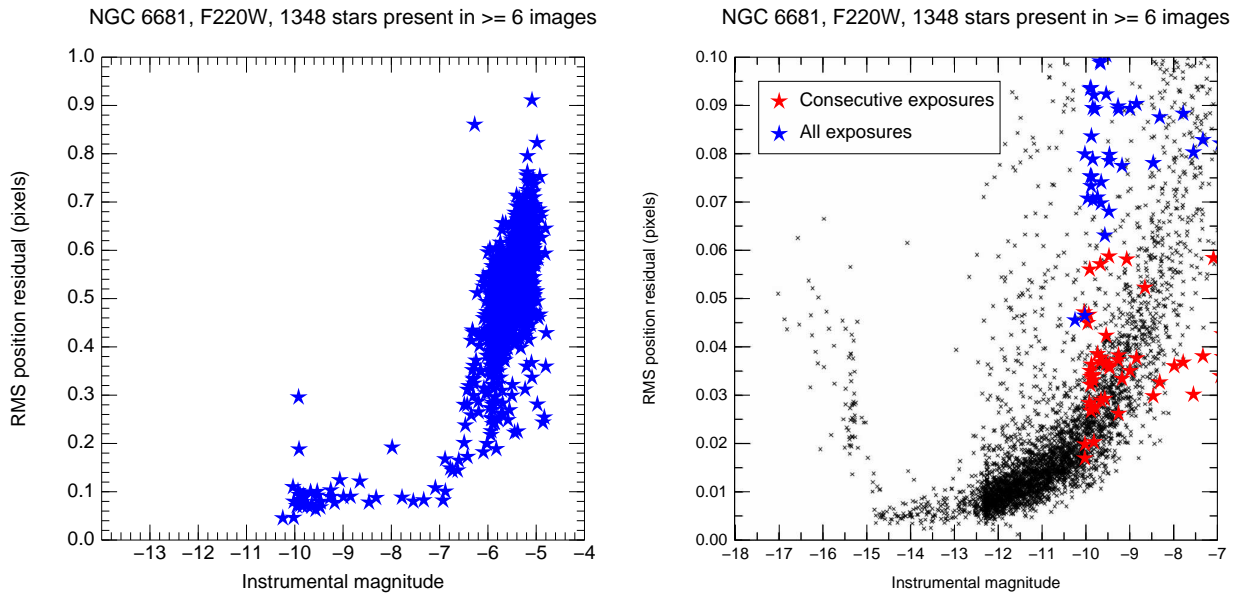


Figure 7: Same as Fig. 5 for NGC 6681 and F220W exposures. The red symbols correspond to the RMS derived by comparing sets of consecutive exposures within the same visit and orientation while the blue ones use all exposures (as in the previous two figures). The instrumental magnitude refers to an exposure time of 70 s.

decreases, as expected. The most likely explanation for the effect on the NGC 6681 F220W data is the small number of bright stars in this case (there are only 45 stars with $m_{\text{ins}} < -7.0$ and none with $m_{\text{ins}} < -10.3$; in the other three cases those numbers are ~ 200 and ~ 20 , respectively), which does not allow for the average-position calculation algorithm to determine the linear transformation with an accuracy as large as in the other three cases (note how the RMS residuals from consecutive exposures are not affected by this issue).

- The NGC 6681 F250W shows a significantly higher accuracy for the RMS derived from consecutive exposures than for the one derived from all exposures. The likely explanation here is the absence of a filter-dependent table for the F250W geometric distortion solution. The observed effect is of the order of 0.03 pixels, which is a reasonable value (compare with Table 4 in Anderson and King 2004 and see also below).
- For NGC 604, the overall appearance of the right panels is similar to that of the F475W results except for the brightest stars ($m_{\text{ins}} \approx -11$), which appear to have significantly higher uncertainties (≈ 0.04 pixels vs. ≈ 0.01 pixels). For the F250W data this could be the same effect (absence of a filter-dependent table) as for the NGC 6681 F250W case, but a similar issue is seen for F220W, where a table is indeed used. There are two possible explanations: inaccuracies in the geometric distortion at the level of a few hundredths of a pixel (either intrinsic or as a result of temporal evolution, see Anderson 2007 for an analysis of this effect on the WFC) or absence of very bright stars ($m_{\text{ins}} \approx -14$) which limit the accuracy of the calculated linear transformations (i.e. the same effect seen for the NGC 6681 F220W data but with an amplitude $\sim 1/3$ smaller).

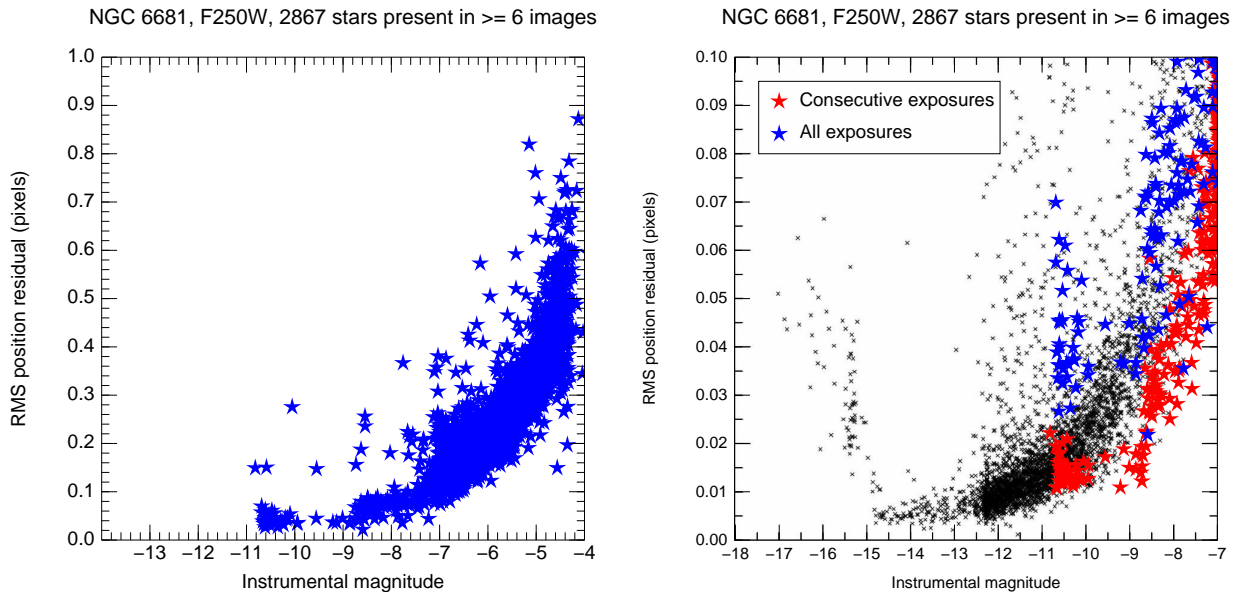


Figure 8: Same as Fig. 7 for NGC 6681 and F250W exposures. The instrumental magnitude refers to an exposure time of 70 s.

Despite these minor issues, the transformations and distortion solution of the HRC appear to be good enough to establish accurate astrometric fields from our data. I selected the brightest stars ($m_{ST,F250W} \leq 20.0$ for NGC 604, $m_{ST,F250W} \leq 19.5$ for NGC 6681) in order to eliminate those objects with large uncertainties⁴ and listed the coordinates in Tables 3 and 4. The coordinates are in the J2000.0 epoch. The NGC 604 coordinates are an average of the F220W and F250W results while for NGC 6681 I have used only the F250W data, given their higher precision. Typical uncertainties for the positions in Tables 3 and 4 are 1 mas (brightest objects) and 3 mas (dimmiest objects)⁵. A nearby bright star present in WFPC2 frames (Maíz Apellániz et al. 2004) has been used to introduce a global shift in the NGC 604 coordinates, thus making them accurate in an absolute sense at the 0.1'' level. No such shift was applied to the NGC 6681 data, so it is possible that the absolute coordinates have a displacement of the order of 1''. The ST magnitudes listed in Tables 3 and 4 should be accurate only at the 0.1 magnitude level, since at the time of this writing there are no L-flats available for either F220W or F250W and because no CTE correction has been applied.

An additional limitation to the accuracy of the NGC 6681 data is the existence of proper and, in binary systems, orbital motions. The distance and velocity dispersion of that globular cluster should produce internal motions at the 0.1 mas/a level and should be detectable in our data. Indeed, some stars show this effect (Fig. 9), which may also contribute to the difference between the uncertainties derived from consecutive and all exposures for the NGC 6681 F250W data. Therefore, we conclude that NGC 604, being two orders of magnitude farther away, provides a better long-term choice for an astrometric field.

I have performed one further check of the accuracy of the analysis. Figure 10 shows the difference

⁴If the reader is interested in the coordinates of the lower S/N objects, he/she can contact the author at jmaiz@iaa.es.

⁵These uncertainties are RMS values, i.e the sample standard deviation of the data. If one is confident that the dispersion is purely random and that no systematic effects (e.g. proper motions or geometric distortion inaccuracies) are present, then it is possible to divide those numbers by the square root of the number of exposures to use the standard deviation of the mean as the uncertainty. Therefore, for NGC 604 one may use 0.3 mas and 1 mas, respectively. For NGC 6681, see below regarding proper motions.

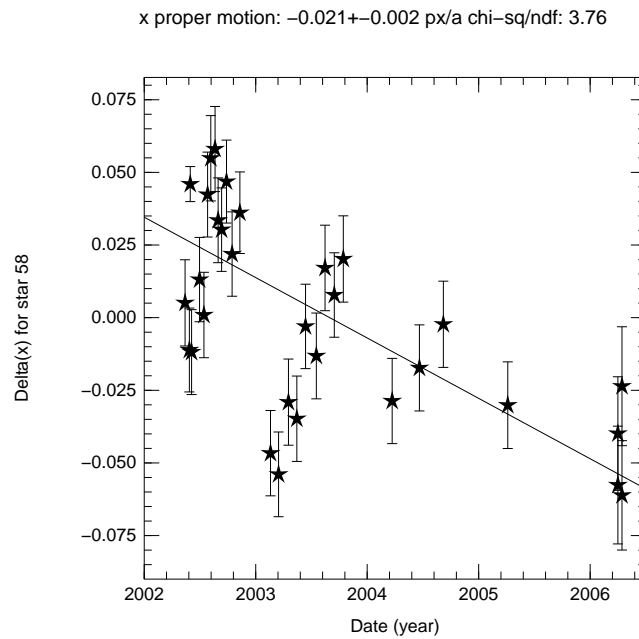


Figure 9: An example of a star with possible proper and orbital motions. The vertical scale is in x DRZ pixels.

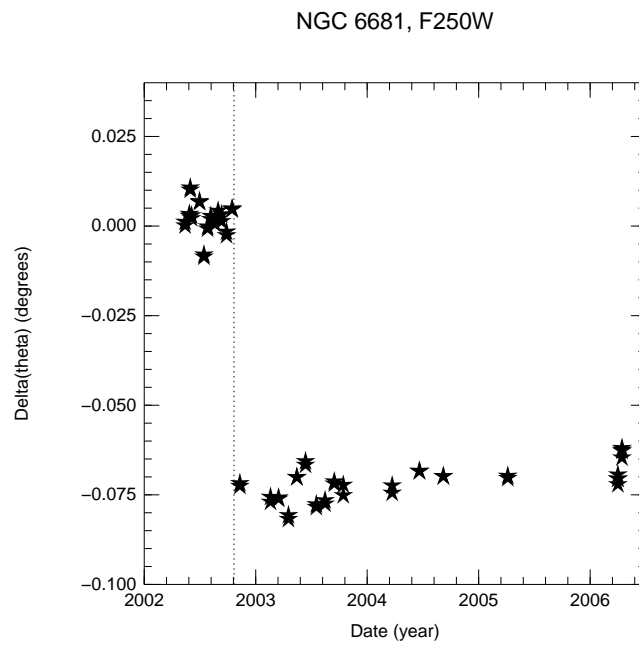


Figure 10: Difference between the header and the measured orientation as a function of time for the NGC 6681 F250W exposures.

between the header and the measured orientation as a function of time for the NGC 6681 F250W exposures, as determined by the parameters of the linear transformation. A clear jump of 0.08 degrees is seen in October

2002 that corresponds to the FGS realignment, as expected. Note, however, that an apparent scatter of the order of 0.005 degrees is seen in the trends observed before and after the FGS realignment. It is possible that scatter is not real but a consequence of the absence of very bright stars, which could be limiting the accuracy of the calculated linear transformations and producing the higher-than-expected uncertainties for bright stars.

I conclude that the data in Tables 3 and 4 can be used as high-accuracy astrometric fields in the UV, with the NGC 604 field being preferred for its richness of bright stars (especially in the FUV) and its absence of detectable proper/orbital motions at the 0.1 mas/a level. In the process of determining these astrometric fields I have confirmed the stability of the HRC and the validity of the Anderson and King (2004) geometric distortion solution to do long-term astrometry at the 1 mas level. It is my plan to use these fields to improve the existing geometric distortion solution for the three MAMA detectors on HST, the STIS FUV- and NUV-MAMA and the ACS SBC.

I would like to thank Jay Anderson for his help in developing the techniques used in this ISR and for his useful comments on a draft. I also thank Marco Sirianni and the rest of the ACS team for their comments.

REVISION 4 October 2007: Two months after initially publishing this ISR a typo in the computer code was found at the point where the global coordinate shift for NGC 604 was applied. As a result, the absolute astrometry had an offset of almost 1", which has been corrected in the current version.

Bibliography

- Anderson, J. 2007, *ACS Instrument Science Report 2007-08 (STScI: Baltimore)*
- Anderson, J. and King, I. R. 2004, *ACS Instrument Science Report 2004-15 (STScI: Baltimore)*
- Anderson, J. and King, I. R. 2006, *ACS Instrument Science Report 2006-01 (STScI: Baltimore)*
- Drissen, L., Moffat, A. F. J., and Shara, M. M. 1993, *AJ* **105**, 1400
- Harris, W. E. 1996, *AJ* **112**, 1487
- Hunter, D. A., Baum, W. A., O'Neil, Jr., E. J., and Lynds, R. 1996, *ApJ* **456**, 174
- Maíz Apellániz, J., Pérez, E., and Mas-Hesse, J. M. 2004, *AJ* **128**, 1196
- Maíz Apellániz, J. and Úbeda, L. 2004, *STIS Instrument Science Report 2004-01 (STScI: Baltimore)*

Table 3. NGC 604 astrometric field data.

| # | RA 1 ^h 34 ^m + | dec 30° 46' + | m_{ST} F250W | # | RA 1 ^h 34 ^m + | dec 30° 46' + | m_{ST} F250W | # | RA 1 ^h 34 ^m + | dec 30° 46' + | m_{ST} F250W |
|----|--|------------------|-------------------|-----|--|------------------|-------------------|-----|--|------------------|-------------------|
| 1 | 32.717793 | 69.52561 | 14.7 | 51 | 32.555811 | 55.96107 | 17.8 | 101 | 31.769727 | 64.88008 | 18.6 |
| 2 | 32.421560 | 59.01234 | 15.0 | 52 | 33.240209 | 54.66074 | 17.8 | 102 | 32.679891 | 65.32767 | 18.6 |
| 3 | 33.076165 | 58.87771 | 15.6 | 53 | 33.568684 | 63.91171 | 17.8 | 103 | 33.414842 | 55.60044 | 18.6 |
| 4 | 32.311865 | 65.74607 | 15.8 | 54 | 33.295222 | 54.04217 | 17.8 | 104 | 33.172668 | 54.98746 | 18.6 |
| 5 | 32.610397 | 63.59869 | 15.9 | 55 | 32.036998 | 56.91476 | 17.8 | 105 | 33.521601 | 66.77396 | 18.6 |
| 6 | 32.217329 | 62.65050 | 16.0 | 56 | 31.945571 | 49.70745 | 17.8 | 106 | 32.702173 | 74.22079 | 18.6 |
| 7 | 32.377071 | 64.92499 | 16.0 | 57 | 33.302575 | 59.75878 | 17.9 | 107 | 32.352189 | 58.87904 | 18.7 |
| 8 | 32.571983 | 65.86124 | 16.0 | 58 | 33.396032 | 67.49206 | 17.9 | 108 | 32.731552 | 67.45632 | 18.7 |
| 9 | 33.537800 | 64.72609 | 16.1 | 59 | 32.955017 | 66.91885 | 17.9 | 109 | 33.193523 | 70.46106 | 18.7 |
| 10 | 32.763622 | 67.32248 | 16.2 | 60 | 33.307493 | 60.16128 | 17.9 | 110 | 32.816684 | 63.66196 | 18.7 |
| 11 | 32.652389 | 66.81992 | 16.2 | 61 | 32.703766 | 64.10036 | 18.0 | 111 | 32.104536 | 65.62222 | 18.7 |
| 12 | 32.289142 | 59.68604 | 16.3 | 62 | 32.591733 | 62.77523 | 18.0 | 112 | 32.621324 | 67.47970 | 18.7 |
| 13 | 32.696735 | 67.02612 | 16.3 | 63 | 32.721352 | 66.53314 | 18.0 | 113 | 33.162451 | 69.93321 | 18.7 |
| 14 | 32.608371 | 64.18273 | 16.4 | 64 | 33.087561 | 69.12136 | 18.0 | 114 | 32.587904 | 64.61247 | 18.7 |
| 15 | 33.543104 | 68.59969 | 16.5 | 65 | 32.958578 | 65.17852 | 18.0 | 115 | 32.978760 | 68.87019 | 18.7 |
| 16 | 32.472583 | 63.22302 | 16.5 | 66 | 33.303254 | 53.84408 | 18.1 | 116 | 32.337096 | 58.21138 | 18.8 |
| 17 | 32.090578 | 65.81622 | 16.5 | 67 | 32.982123 | 58.78947 | 18.1 | 117 | 31.423262 | 65.88225 | 18.8 |
| 18 | 32.284969 | 65.49587 | 16.7 | 68 | 32.647638 | 66.70621 | 18.1 | 118 | 32.616096 | 61.19297 | 18.8 |
| 19 | 32.656084 | 55.27386 | 16.7 | 69 | 32.270359 | 55.03894 | 18.1 | 119 | 32.667578 | 66.80528 | 18.8 |
| 20 | 32.251087 | 62.31049 | 16.7 | 70 | 32.581739 | 62.96717 | 18.1 | 120 | 33.262133 | 67.11934 | 18.8 |
| 21 | 32.413586 | 65.58170 | 16.8 | 71 | 32.965141 | 57.58454 | 18.2 | 121 | 32.652756 | 54.73838 | 18.8 |
| 22 | 33.598966 | 64.57992 | 16.8 | 72 | 32.423901 | 59.14025 | 18.2 | 122 | 32.054798 | 61.56427 | 18.8 |
| 23 | 32.157867 | 61.68261 | 16.8 | 73 | 33.061947 | 54.44918 | 18.2 | 123 | 32.730794 | 67.83161 | 18.8 |
| 24 | 32.535362 | 59.53634 | 16.9 | 74 | 32.475099 | 63.45142 | 18.2 | 124 | 32.619152 | 65.69435 | 18.8 |
| 25 | 33.191955 | 64.56020 | 16.9 | 75 | 32.429293 | 62.50564 | 18.2 | 125 | 33.269821 | 56.18185 | 18.8 |
| 26 | 32.482203 | 60.02329 | 17.0 | 76 | 32.417869 | 65.30479 | 18.2 | 126 | 32.843826 | 63.75018 | 18.8 |
| 27 | 32.832050 | 50.58799 | 17.1 | 77 | 32.345479 | 61.10642 | 18.3 | 127 | 33.060708 | 54.11460 | 18.8 |
| 28 | 32.584863 | 65.94017 | 17.1 | 78 | 33.055146 | 65.22567 | 18.3 | 128 | 32.317728 | 59.30772 | 18.8 |
| 29 | 32.111416 | 58.40432 | 17.1 | 79 | 32.737418 | 77.17296 | 18.3 | 129 | 32.676361 | 66.42472 | 18.8 |
| 30 | 33.542024 | 65.41017 | 17.1 | 80 | 32.026719 | 70.28934 | 18.3 | 130 | 32.567566 | 55.11270 | 18.9 |
| 31 | 32.368623 | 61.41992 | 17.1 | 81 | 32.360108 | 63.29997 | 18.3 | 131 | 32.490107 | 66.08232 | 18.9 |
| 32 | 32.471773 | 66.65797 | 17.2 | 82 | 32.832246 | 70.32964 | 18.3 | 132 | 32.566893 | 55.72927 | 18.9 |
| 33 | 31.961614 | 62.86559 | 17.2 | 83 | 32.677961 | 65.16141 | 18.3 | 133 | 32.573704 | 66.85386 | 18.9 |
| 34 | 32.911265 | 52.97126 | 17.3 | 84 | 32.532929 | 65.38775 | 18.4 | 134 | 32.967891 | 70.12072 | 18.9 |
| 35 | 32.454110 | 63.90694 | 17.3 | 85 | 32.420975 | 61.43664 | 18.4 | 135 | 32.305048 | 59.07539 | 18.9 |
| 36 | 33.005953 | 64.83629 | 17.3 | 86 | 33.466893 | 65.34103 | 18.4 | 136 | 32.716408 | 60.71090 | 18.9 |
| 37 | 33.222704 | 55.69255 | 17.3 | 87 | 32.657443 | 69.06327 | 18.5 | 137 | 32.736852 | 66.82829 | 19.0 |
| 38 | 33.251114 | 60.13757 | 17.3 | 88 | 32.702939 | 50.56744 | 18.5 | 138 | 33.428261 | 56.38349 | 19.0 |
| 39 | 32.395523 | 58.41936 | 17.4 | 89 | 32.684552 | 67.97841 | 18.5 | 139 | 32.520447 | 68.83226 | 19.0 |
| 40 | 32.520306 | 58.55686 | 17.5 | 90 | 33.458512 | 57.04199 | 18.5 | 140 | 32.633334 | 66.11767 | 19.0 |
| 41 | 32.695656 | 66.74804 | 17.5 | 91 | 33.363303 | 55.82237 | 18.5 | 141 | 33.411472 | 52.93647 | 19.1 |
| 42 | 32.855660 | 67.29099 | 17.5 | 92 | 32.636641 | 63.41395 | 18.5 | 142 | 32.563795 | 73.96834 | 19.1 |
| 43 | 32.624395 | 66.16063 | 17.5 | 93 | 32.159535 | 63.57277 | 18.5 | 143 | 33.420441 | 56.95939 | 19.1 |
| 44 | 32.566530 | 65.95987 | 17.5 | 94 | 31.826025 | 78.56597 | 18.5 | 144 | 32.668068 | 63.29174 | 19.1 |
| 45 | 32.849225 | 71.51536 | 17.6 | 95 | 32.320745 | 61.57408 | 18.5 | 145 | 32.527351 | 58.21186 | 19.1 |
| 46 | 32.746136 | 63.45604 | 17.6 | 96 | 33.008686 | 58.78251 | 18.5 | 146 | 32.298091 | 63.08081 | 19.1 |
| 47 | 33.429919 | 57.14285 | 17.6 | 97 | 32.075386 | 65.04726 | 18.6 | 147 | 32.386676 | 57.45504 | 19.1 |
| 48 | 33.014490 | 59.26698 | 17.6 | 98 | 32.396020 | 62.33965 | 18.6 | 148 | 32.523357 | 64.46760 | 19.1 |
| 49 | 32.736326 | 68.04175 | 17.7 | 99 | 33.461580 | 54.84378 | 18.6 | 149 | 32.913965 | 64.34593 | 19.1 |
| 50 | 33.146174 | 58.16102 | 17.8 | 100 | 33.079547 | 63.45634 | 18.6 | 150 | 32.605306 | 67.67437 | 19.1 |

Table 3 (continued). NGC 604 astrometric field data.

| # | RA 1 ^h 34 ^m + | dec 30° 46' + | m_{ST} F250W | # | RA 1 ^h 34 ^m + | dec 30° 46' + | m_{ST} F250W | # | RA 1 ^h 34 ^m + | dec 30° 46' + | m_{ST} F250W |
|-----|--|------------------|-------------------|-----|--|------------------|-------------------|-----|--|------------------|-------------------|
| 151 | 33.116673 | 63.46851 | 19.2 | 189 | 33.423487 | 53.72027 | 19.5 | 227 | 32.666789 | 65.22927 | 19.8 |
| 152 | 32.995356 | 64.13734 | 19.2 | 190 | 32.755836 | 67.26448 | 19.5 | 228 | 32.961798 | 68.05689 | 19.8 |
| 153 | 33.243821 | 57.64608 | 19.2 | 191 | 33.142589 | 63.35063 | 19.5 | 229 | 33.792823 | 56.40281 | 19.8 |
| 154 | 32.630520 | 63.14362 | 19.2 | 192 | 32.198471 | 61.65535 | 19.6 | 230 | 32.769502 | 51.24300 | 19.8 |
| 155 | 32.312932 | 60.52433 | 19.2 | 193 | 32.333951 | 58.81935 | 19.6 | 231 | 32.539129 | 58.36557 | 19.8 |
| 156 | 33.333236 | 62.24086 | 19.2 | 194 | 32.270324 | 65.54860 | 19.6 | 232 | 33.364349 | 49.42566 | 19.8 |
| 157 | 32.604334 | 69.15019 | 19.2 | 195 | 32.504136 | 63.90915 | 19.6 | 233 | 32.597048 | 64.47468 | 19.8 |
| 158 | 33.117871 | 59.87806 | 19.2 | 196 | 32.372336 | 67.37634 | 19.6 | 234 | 33.412146 | 54.32374 | 19.8 |
| 159 | 32.011816 | 62.22814 | 19.2 | 197 | 33.026234 | 61.60918 | 19.6 | 235 | 32.432073 | 61.44891 | 19.8 |
| 160 | 32.346389 | 61.95646 | 19.2 | 198 | 33.019207 | 69.40290 | 19.6 | 236 | 32.704439 | 67.70779 | 19.8 |
| 161 | 33.066422 | 50.32386 | 19.2 | 199 | 32.236278 | 60.18722 | 19.6 | 237 | 33.252098 | 65.44247 | 19.8 |
| 162 | 32.675872 | 65.44496 | 19.2 | 200 | 32.815984 | 65.56830 | 19.6 | 238 | 32.623074 | 68.13862 | 19.8 |
| 163 | 32.663130 | 65.72639 | 19.3 | 201 | 32.886886 | 70.34860 | 19.6 | 239 | 32.696393 | 67.47316 | 19.9 |
| 164 | 33.529684 | 70.72586 | 19.3 | 202 | 32.910427 | 41.47207 | 19.6 | 240 | 31.669154 | 77.05459 | 19.9 |
| 165 | 32.576912 | 60.72354 | 19.3 | 203 | 31.426128 | 78.88375 | 19.6 | 241 | 32.384519 | 61.26250 | 19.9 |
| 166 | 32.526806 | 60.93231 | 19.3 | 204 | 33.145702 | 59.06088 | 19.6 | 242 | 33.428940 | 54.58017 | 19.9 |
| 167 | 33.451581 | 66.12344 | 19.3 | 205 | 32.477154 | 59.12069 | 19.6 | 243 | 33.385658 | 54.66439 | 19.9 |
| 168 | 33.345202 | 57.63837 | 19.3 | 206 | 32.661007 | 51.25839 | 19.6 | 244 | 33.361668 | 65.17268 | 19.9 |
| 169 | 33.588140 | 65.84012 | 19.3 | 207 | 32.548829 | 64.12924 | 19.7 | 245 | 32.422170 | 66.23470 | 19.9 |
| 170 | 33.048569 | 73.99681 | 19.3 | 208 | 32.269756 | 40.66626 | 19.7 | 246 | 32.795729 | 63.30675 | 19.9 |
| 171 | 32.860041 | 55.59629 | 19.4 | 209 | 32.641758 | 60.57830 | 19.7 | 247 | 33.132432 | 54.65055 | 19.9 |
| 172 | 33.200361 | 77.11240 | 19.4 | 210 | 32.339478 | 63.55479 | 19.7 | 248 | 33.262068 | 75.77199 | 20.0 |
| 173 | 33.280537 | 55.88680 | 19.4 | 211 | 32.603380 | 63.39716 | 19.7 | 249 | 32.263162 | 57.52118 | 20.0 |
| 174 | 32.769293 | 63.84863 | 19.4 | 212 | 32.953000 | 67.86260 | 19.7 | 250 | 32.251696 | 61.32072 | 20.0 |
| 175 | 32.641603 | 51.83999 | 19.4 | 213 | 33.121171 | 59.47959 | 19.7 | 251 | 32.473192 | 59.56549 | 20.0 |
| 176 | 32.330936 | 62.26354 | 19.4 | 214 | 33.007614 | 63.11355 | 19.7 | 252 | 33.414603 | 52.31769 | 20.0 |
| 177 | 32.960841 | 46.38645 | 19.4 | 215 | 33.428635 | 56.56954 | 19.7 | 253 | 33.192089 | 67.83967 | 20.0 |
| 178 | 31.974105 | 62.04931 | 19.4 | 216 | 31.876705 | 62.38586 | 19.7 | 254 | 32.213988 | 62.33870 | 20.0 |
| 179 | 32.791955 | 54.30159 | 19.5 | 217 | 33.484813 | 67.22510 | 19.8 | 255 | 33.135171 | 57.13054 | 20.0 |
| 180 | 31.399650 | 54.78220 | 19.5 | 218 | 32.728098 | 68.26834 | 19.8 | 256 | 32.371241 | 61.63714 | 20.0 |
| 181 | 32.401819 | 59.80950 | 19.5 | 219 | 32.409327 | 57.07132 | 19.8 | 257 | 32.431685 | 63.84123 | 20.0 |
| 182 | 33.020088 | 63.89548 | 19.5 | 220 | 32.743674 | 68.10795 | 19.8 | 258 | 32.571304 | 64.34153 | 20.0 |
| 183 | 32.398997 | 57.41243 | 19.5 | 221 | 33.183372 | 67.59697 | 19.8 | 259 | 32.525721 | 71.10991 | 20.0 |
| 184 | 33.207999 | 53.31070 | 19.5 | 222 | 32.594011 | 63.82717 | 19.8 | 260 | 32.789523 | 55.49292 | 20.0 |
| 185 | 32.182236 | 59.45612 | 19.5 | 223 | 32.180133 | 63.35510 | 19.8 | 261 | 33.630044 | 65.51907 | 20.0 |
| 186 | 33.135214 | 54.21668 | 19.5 | 224 | 32.639387 | 65.86835 | 19.8 | 262 | 32.649872 | 73.35506 | 20.0 |
| 187 | 33.023419 | 63.11215 | 19.5 | 225 | 33.291443 | 70.58387 | 19.8 | | | | |
| 188 | 32.920993 | 69.09055 | 19.5 | 226 | 32.418825 | 63.37265 | 19.8 | | | | |

Table 4. NGC 6681 astrometric field data.

| # | RA 18 ^h 43 ^m + | dec −32° 17′ + | m_{ST} F250W | # | RA 18 ^h 43 ^m + | dec −32° 17′ + | m_{ST} F250W | # | RA 18 ^h 43 ^m + | dec −32° 17′ + | m_{ST} F250W |
|----|---|-------------------|-------------------|----|---|-------------------|-------------------|-----|---|-------------------|-------------------|
| 1 | 13.121868 | 44.46000 | 16.0 | 49 | 12.200782 | 26.25134 | 18.1 | 97 | 13.009648 | 23.25710 | 18.9 |
| 2 | 13.558360 | 35.75421 | 16.1 | 50 | 13.841436 | 25.73742 | 18.2 | 98 | 12.263997 | 15.33049 | 18.9 |
| 3 | 13.061846 | 16.16410 | 16.1 | 51 | 12.703568 | 31.89232 | 18.2 | 99 | 12.673192 | 35.79141 | 19.0 |
| 4 | 12.945839 | 26.06638 | 16.2 | 52 | 12.911361 | 30.39058 | 18.2 | 100 | 13.086195 | 42.15176 | 19.0 |
| 5 | 12.510109 | 38.77682 | 16.2 | 53 | 12.804464 | 36.23853 | 18.2 | 101 | 12.863976 | 31.31022 | 19.0 |
| 6 | 13.160029 | 23.41762 | 16.2 | 54 | 13.109778 | 20.36792 | 18.2 | 102 | 12.614087 | 13.32399 | 19.0 |
| 7 | 12.353232 | 22.84667 | 16.2 | 55 | 12.988439 | 14.07230 | 18.2 | 103 | 13.276317 | 28.90240 | 19.1 |
| 8 | 13.467278 | 20.00456 | 16.2 | 56 | 11.896022 | 25.73052 | 18.2 | 104 | 12.770918 | 31.61028 | 19.1 |
| 9 | 13.016384 | 34.48359 | 16.2 | 57 | 13.021804 | 26.31683 | 18.3 | 105 | 13.610475 | 20.10618 | 19.1 |
| 10 | 13.730866 | 41.82659 | 16.2 | 58 | 12.782085 | 31.60420 | 18.3 | 106 | 12.465210 | 34.36672 | 19.1 |
| 11 | 14.023057 | 41.16347 | 16.2 | 59 | 12.817820 | 30.71071 | 18.3 | 107 | 13.128905 | 37.67851 | 19.1 |
| 12 | 13.544142 | 44.50542 | 16.2 | 60 | 12.705130 | 40.50931 | 18.3 | 108 | 12.807901 | 30.74984 | 19.2 |
| 13 | 12.807306 | 25.33684 | 16.2 | 61 | 13.040943 | 38.77875 | 18.3 | 109 | 13.029815 | 25.84472 | 19.2 |
| 14 | 13.600251 | 16.70653 | 16.2 | 62 | 11.959255 | 38.62252 | 18.3 | 110 | 12.460841 | 15.76427 | 19.2 |
| 15 | 11.955681 | 27.58007 | 16.2 | 63 | 12.976792 | 32.85117 | 18.3 | 111 | 12.876897 | 23.39082 | 19.2 |
| 16 | 13.381662 | 22.76167 | 16.3 | 64 | 12.280148 | 30.34821 | 18.3 | 112 | 12.870140 | 32.26833 | 19.2 |
| 17 | 12.387632 | 48.28847 | 16.3 | 65 | 12.620508 | 40.52951 | 18.4 | 113 | 12.549517 | 18.13723 | 19.2 |
| 18 | 12.287744 | 38.24983 | 16.3 | 66 | 12.903877 | 18.89836 | 18.4 | 114 | 12.503670 | 34.53366 | 19.2 |
| 19 | 12.249488 | 30.65285 | 16.3 | 67 | 12.872024 | 31.89644 | 18.4 | 115 | 12.405817 | 26.62964 | 19.2 |
| 20 | 11.996445 | 32.35547 | 16.3 | 68 | 13.154711 | 30.10158 | 18.4 | 116 | 12.816575 | 30.14801 | 19.3 |
| 21 | 13.143612 | 35.02711 | 16.4 | 69 | 12.022222 | 37.91423 | 18.4 | 117 | 12.796610 | 31.65929 | 19.3 |
| 22 | 12.508075 | 17.82186 | 16.4 | 70 | 12.581999 | 48.59265 | 18.4 | 118 | 12.758546 | 28.97306 | 19.3 |
| 23 | 11.971214 | 30.83099 | 16.4 | 71 | 13.221246 | 33.74399 | 18.5 | 119 | 12.405676 | 14.83515 | 19.4 |
| 24 | 12.329978 | 27.17338 | 16.4 | 72 | 13.357093 | 28.15891 | 18.5 | 120 | 13.891507 | 26.61102 | 19.4 |
| 25 | 13.092540 | 25.04352 | 16.5 | 73 | 12.692965 | 26.73377 | 18.5 | 121 | 12.728453 | 30.88727 | 19.4 |
| 26 | 12.294293 | 31.79874 | 16.5 | 74 | 13.054707 | 33.07967 | 18.5 | 122 | 12.824991 | 36.01734 | 19.4 |
| 27 | 12.565495 | 34.65015 | 16.5 | 75 | 13.046308 | 27.96147 | 18.5 | 123 | 12.330980 | 23.92125 | 19.4 |
| 28 | 12.924348 | 26.19555 | 16.6 | 76 | 12.081218 | 15.74694 | 18.5 | 124 | 13.155571 | 30.76246 | 19.4 |
| 29 | 13.217493 | 25.45625 | 16.6 | 77 | 12.673837 | 31.90006 | 18.5 | 125 | 13.696418 | 26.49110 | 19.4 |
| 30 | 13.377944 | 22.02920 | 16.6 | 78 | 12.629943 | 23.91071 | 18.5 | 126 | 12.634152 | 24.17935 | 19.4 |
| 31 | 13.014734 | 29.24217 | 16.6 | 79 | 12.668415 | 33.42087 | 18.6 | 127 | 12.306088 | 21.92084 | 19.4 |
| 32 | 12.810337 | 27.97660 | 16.7 | 80 | 11.492721 | 35.83757 | 18.6 | 128 | 12.138318 | 26.11825 | 19.5 |
| 33 | 12.631940 | 30.72069 | 16.7 | 81 | 12.103265 | 26.46710 | 18.7 | 129 | 12.399682 | 26.32783 | 19.5 |
| 34 | 13.503898 | 33.23989 | 16.8 | 82 | 12.897886 | 34.57456 | 18.7 | 130 | 12.576935 | 39.90143 | 19.5 |
| 35 | 12.686839 | 22.93006 | 16.9 | 83 | 12.721779 | 21.06086 | 18.7 | 131 | 13.091584 | 33.54737 | 19.5 |
| 36 | 13.937130 | 39.27026 | 16.9 | 84 | 11.682730 | 26.59207 | 18.7 | 132 | 12.384035 | 28.75120 | 19.5 |
| 37 | 13.371528 | 24.99136 | 17.3 | 85 | 11.877046 | 45.80444 | 18.7 | 133 | 12.717087 | 31.08541 | 19.5 |
| 38 | 13.402125 | 15.55495 | 17.3 | 86 | 12.306247 | 34.58071 | 18.8 | 134 | 12.610234 | 29.11917 | 19.5 |
| 39 | 12.102528 | 27.17816 | 17.6 | 87 | 12.486797 | 21.87724 | 18.8 | 135 | 11.841970 | 37.34487 | 19.5 |
| 40 | 12.252387 | 26.75944 | 17.7 | 88 | 13.280811 | 21.83066 | 18.8 | 136 | 12.496950 | 32.50279 | 19.5 |
| 41 | 12.514002 | 32.63603 | 17.8 | 89 | 11.984771 | 31.39214 | 18.8 | 137 | 13.728684 | 24.18138 | 19.5 |
| 42 | 11.988635 | 27.36462 | 18.0 | 90 | 12.471791 | 33.96993 | 18.9 | 138 | 13.834821 | 30.00414 | 19.5 |
| 43 | 13.166275 | 28.40547 | 18.0 | 91 | 12.395103 | 38.63243 | 18.9 | 139 | 12.452599 | 23.09211 | 19.5 |
| 44 | 12.428084 | 46.30086 | 18.1 | 92 | 12.115547 | 25.81191 | 18.9 | 140 | 12.814818 | 33.88595 | 19.5 |
| 45 | 13.723210 | 17.20295 | 18.1 | 93 | 13.009636 | 32.60800 | 18.9 | 141 | 13.698363 | 26.96457 | 19.5 |
| 46 | 13.181013 | 37.68670 | 18.1 | 94 | 12.175168 | 20.95547 | 18.9 | 142 | 12.545392 | 12.29171 | 19.5 |
| 47 | 12.858356 | 33.44178 | 18.1 | 95 | 12.744022 | 17.10641 | 18.9 | 143 | 12.819176 | 43.45388 | 19.5 |
| 48 | 12.073580 | 29.47395 | 18.1 | 96 | 12.719999 | 44.47515 | 18.9 | | | | |